NASA galactic cosmic radiation environment model: Badhwar - O'Neill (2014)

S. Golge[*a,b], **P. M. O'Neill**[c], **and T. C. Slaba**[d]

[a]*University of Houston, Houston, Texas 77004, USA*

[b]*Space Radiation Analysis Group, NASA Johnson Space Center, Houston, Texas 77058, USA*

[c]*EEE Parts and Radiation Group, NASA Johnson Space Center, Houston, Texas 77058, USA*

[d]*Space Radiation Group, NASA Langley Research Center, Hampton, Virginia 23681, USA*

The Badhwar-O'Neill (BON) Galactic Cosmic Ray (GCR) flux model has been used by NASA to certify microelectronic systems and in the analysis of radiation health risks for human space flight missions. Of special interest to NASA is the kinetic energy region below 4.0 GeV/n due to the fact that exposure from GCR behind shielding (e.g., inside a space vehicle) is heavily influenced by the GCR particles from this energy domain. The BON model numerically solves the Fokker-Planck differential equation to account for particle transport in the heliosphere due to diffusion, convection, and adiabatic deceleration under the assumption of a spherically symmetric heliosphere. The model utilizes a comprehensive database of GCR measurements from various particle detectors to determine boundary conditions. By using an updated GCR database and improved model fit parameters, the new BON model (BON14) is significantly improved over the previous BON models for describing the GCR radiation environment of interest to human space flight.

The 34th International Cosmic Ray Conference,
30 July- 6 August, 2015
The Hague, The Netherlands

---

[*]Speaker. Corresponding author e-mail: serkan.golge@nasa.gov

1. Introduction

It is well known with many years of research and as documented in the literature that the ionizing nature of Galactic Cosmic Ray (GCR) particles poses a potential health risk for crew members in space, particularly for future long-term missions in free-space [1–3]. Long-term exposure to mixed (both low and high) Linear Energy Transfer (LET) GCR radiation significantly increases the Risk of Exposure Induced Cancer (REIC) and Risk of Exposure Induced Death (REID) [1–3]. Another significant concern arises from the interaction of GCR particles with the electronics inside and outside of a spacecraft. Energetic GCR particles may deposit energy in electronics, e.g., microprocessors, memory units, sufficient to cause memory bit flips and latch-up, which are generically called Single Event Effects (SEE) [4, 5].

In order to evaluate the potential risks induced by the GCR ions, the Badhwar-O'Neill (BON) GCR flux simulation model [6–10] has been developed to numerically solve the Fokker-Planck (FP) equation. The BON model takes into account diffusion, convection, and adiabatic deceleration within the heliosphere and provides the flux of GCR particles of a given charge, Z, as a function of energy near earth ~ 1 astronomical units (AU) in free-space beyond the Earth's magnetosphere. The solution is obtained under the assumptions of a quasi-steady state and a spherically symmetric interplanetary medium [11, 12]. With these assumptions, the FP equation can be written as [13]:

$$\frac{1}{r^2}\frac{\partial}{\partial r}(r^2 V_s U) - \frac{1}{3}\left[\frac{1}{r^2}\frac{\partial}{\partial r}(r^2 V_s)\right]\left[\frac{\partial}{\partial T}(\alpha T U)\right] = \frac{1}{r^2}\frac{\partial}{\partial r}\left(r^2 \kappa \frac{\partial U}{\partial r}\right) \tag{1.1}$$

where r is the radial position in units of AU; T is the kinetic energy (MeV/n); $U(r,T)$ is the GCR flux, $V_s(r)$ the solar wind speed (~ 400 km/s); $\kappa(r,T)$ the particle diffusion coefficient tensor; and $\alpha(T) = (T + 2E_0)/(T + E_0)$, with E_0 being the rest energy per nucleon ($E_p \sim 938$ MeV/n) of the GCR particle. The solution also assumes that at a boundary distance $r = R_b$, modulation of $U(r,T)$ is negligible, and therefore provides the boundary condition at $U(R_b, T) = U_0$ as a known quantity. This quantity, U_0, is ion specific and parametrically described by several free parameters, which are known as Local Interstellar (LIS) parameters.

1.1 Description of the LIS parameters in BON14

At a distance well outside of the solar system, around $R_b = 100$ AU, the GCR modulation due to the turbulent solar wind and heliospheric magnetic field is negligible and therefore each GCR ion energy-flux spectrum is assumed to be constant. This constant GCR field is referred to as the LIS flux spectrum (U_0) and represents one of the boundary conditions for the BON. The LIS flux for each GCR ion has the following parametric relationship as a function of charge (Z) and kinetic energy:

$$U_0(Z, T)\big|_{R_b=100AU} = j_0(Z)(T_N + E_0)^{\gamma(Z)}\beta_N^{-1}\beta^{\delta(Z)}(T + E_0)^{-\gamma(Z)} \tag{1.2}$$

where $j_0, \delta,$ and γ are free parameters for each GCR ion, $\beta = v/c$ is the velocity of the ion relative to the speed of the light, and β_N is the relative velocity at $T_N = 35$ GeV/n (selected arbitrarily for fitting).

The LIS parameters are formulated by using the GCR measurement data from detectors at or near 1 AU; e.g., satellite and balloon measurements. In the model, the flux of any ion beyond nickel (Z > 28) is obtained by scaling from the silicon result. In BON14, as opposed to the previous BON releases, we have modified the LIS parameters, j_0, δ, and γ, driven by a sensitivity study by using several metrics. For a detailed description of the sensitivity analysis, please see the referenced publication series by T. Slaba et al. [14–16].

One of the major results of this study was that for the differential effective dose rate as a function of kinetic energy behind 20 g/cm^2 of aluminum shielding at a period of minimal sun activity, GCR ions in the energy domain between 0.5 GeV/n and 4.0 GeV/n account for most of the exposure. As presented in the study, H and He with boundary energy (BE) less than 0.5 GeV/n induce approximately 9% of the total effective dose. GCR ions with Z > 2 and BE less than 0.5 GeV/n induce less than 4%, while all GCR ions from hydrogen (Z=1) to nickel (Z=28) with BE between 0.5 GeV/n and 4.0 GeV/n induce $\sim$ 66% of the total effective dose behind 20 g/cm^2 aluminium shielding.

Based on the results of that study, the new LIS parameters are fitted to the GCR data, in such a way that allowed a range of parameter combinations to be evaluated to minimize the uncertainty and relative difference between GCR measurements and the model. The updated LIS parameters for each of the corresponding ions from hydrogen to nickel are shown in Table 1.

1.2 Selection of GCR data

In this revision of the BON model, BON14, we have included the GCR data beyond 1970, which spans Solar Cycles 20 to 24 (to date). A comprehensive table that represents the entire GCR measurements used for the BON14 is presented in [10, 16]. In the past, the LIS parameters of the BON were uniquely influenced by measurements from the Cosmic Ray Isotope Spectrometer (CRIS) on the NASA Advanced Composition Explorer (ACE) spacecraft [17]. The CRIS instrument is currently measuring the flux of ions and their isotopes from boron (Z=5) to nickel (Z=28), where the lowest and highest kinetic energy measurements are ion specific. CRIS provides kinetic energy of GCR isotopes between $\sim$ 50 - 500 MeV/n. In the BON14, greater emphasis was placed on the higher kinetic energies, a region not covered by CRIS. Nonetheless, we show that the updated model still accurately represents the lower energy regions.

Table 1: The LIS parameters that are used in the BON14 shown for each ion.

Z	γ	δ	j_0
1	2.75	-2.82	9.50×10^{-4}
2	2.80	-2.00	4.53×10^{-5}
3	3.21	-0.69	6.37×10^{-8}
4	2.93	1.50	1.20×10^{-7}
5	3.00	-0.40	2.40×10^{-7}
6	2.70	-2.00	1.60×10^{-6}
7	2.95	-0.60	2.65×10^{-7}
8	2.73	-1.90	1.50×10^{-6}
9	3.08	0.40	1.63×10^{-8}
10	2.75	-1.60	2.35×10^{-7}
11	2.73	-1.80	4.60×10^{-8}
12	2.70	-2.40	3.03×10^{-7}
13	2.75	-1.40	5.30×10^{-8}
14	2.65	-2.40	2.65×10^{-7}
15	3.15	2.00	5.68×10^{-9}
16	2.70	-1.00	5.78×10^{-8}
17	3.13	2.00	5.99×10^{-9}
18	2.90	0.60	1.68×10^{-8}
19	3.13	0.80	7.90×10^{-9}
20	2.75	-1.60	3.23×10^{-8}
21	3.15	0.40	3.50×10^{-9}
22	3.00	-0.50	1.44×10^{-8}
23	3.00	-0.50	7.14×10^{-9}
24	2.90	-1.00	1.78×10^{-8}
25	2.80	-1.00	1.39×10^{-8}
26	2.60	-2.40	2.00×10^{-7}
27	2.60	-2.50	1.11×10^{-9}
28	2.55	-2.40	1.19×10^{-8}

3

2. Comparison of BON14 to GCR measurements

In Fig. 1, the differential flux for H ion as a function of energy for several GCR measurements, AMS (Alcaraz et al., 2000) [18], IMAX (Menn et al., 2000) [19] , and PAMELA (Adriani et al., 2011) [20], compared with the BON14 model for the same measurement periods is shown. The solid black line in the figure (LIS-BON14) represents the LIS flux for H. The energy axis is magnified in the 0.1-10 GeV/n region and re-plotted in the inset figure.
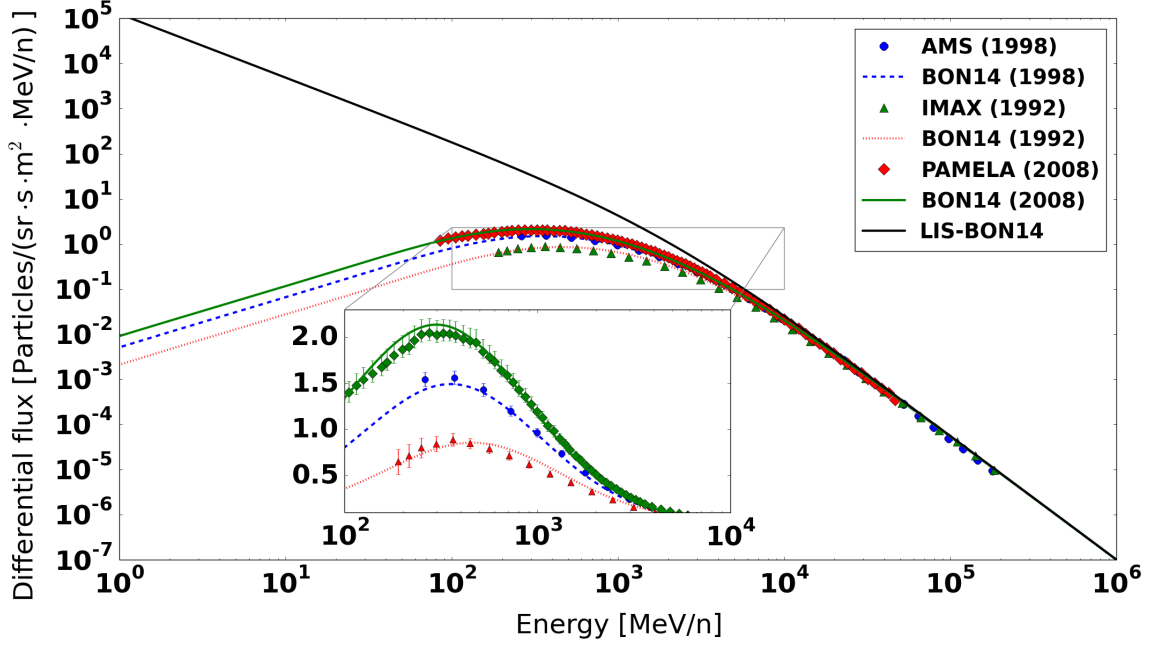

Figure 1: The differential flux for H ions as a function of energy is shown for various GCR measurements, AMS (1998), IMAX (1992), and PAMELA (2008). Those measurements are compared with BON14 for the same measurement periods. The solid black line (LIS-BON14) represents the LIS flux for H ion at R=100 AU. The energy axis is magnified in the 0.1-10 GeV/n region and replotted in the inset figure.

In this paper, we report the comparison of BON14 with the GCR measurement data by evaluating the relative differences between both measurements and the model. A comprehensive study including model uncertainty analysis comparison of the previous BON models (BON10 and BON11) with the current model was reported elsewhere [10]. The relative difference, Rd, is a measurement between the GCR measurement data and the BON model that allows us to find where the model underpredicts or overpredicts the measured GCR flux. Rd is defined as follows:

$$Rd = \frac{1}{N} \sum_{k=1}^{N} \frac{Model_k - Data_k}{Data_k},$$

(2.1)

where N is the number of measurements. The average of the residual Rd does not provide a complete picture of the model versus measurement agreement, as the quantity may end up in the vicinity of zero due to positive-negative cancellation effect. Therefore, we also used the average absolute relative difference, $|Rd|$, to determine the overall difference between the model and the
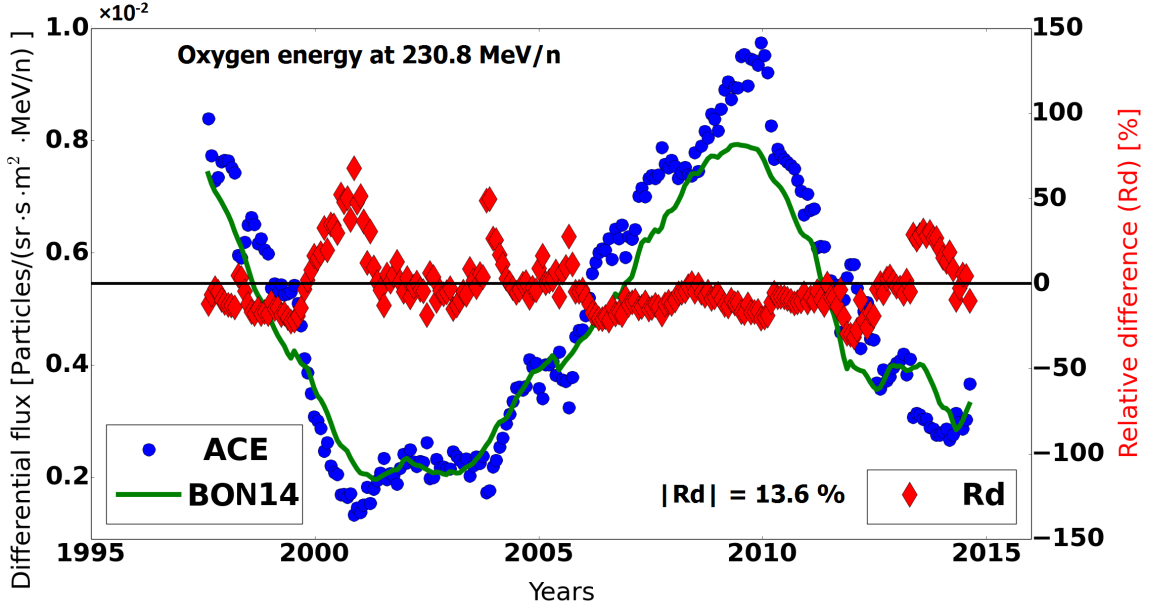
Figure 2: The 27-day average differential flux for O ions at 230.8 MeV/n from ACE/CRIS (circle) as a function of date is compared with BON14 (solid line). On the right axis their *Rd* is shown (diamond).

GCR measurement database, which can be described as follows:

$$|Rd| = \frac{1}{N} \sum_{k=1}^{N} \frac{|Model_k - Data_k|}{Data_k} \qquad (2.2)$$

The latter metric better quantifies the spread in model errors and may be used as a quality check for the model. In Fig. 2, the differential flux averaged over 27 days for O ions at 230.8 MeV/n from ACE/CRIS (circle) as a function of date is compared with BON14. For this particular energy bin, $|Rd|$ is calculated as 13.6%.

In addition, we compared BON14 with the previously released version, BON11, in the energy region of interest. In Fig. 3, comparisons of the average of the integrated differential flux for H, He, O, and Fe ions for all GCR data, excluding ACE/CRIS data, with BON11 and BON14 models are shown. In these figures, we separated the data into two energy regions to simplify comparisons, where they represent lower energy bins (< 4.0 GeV/n) and higher energy bins (≥ 4.0 GeV/n). In those plots, we define the average flux ($< U >$) as the integral of the differential flux (dU/dE) over all energy bins, which is given by the following equation:

$$< U > = \frac{1}{N_{bin}} \int \frac{dU}{dE} dE, \qquad (2.3)$$

where N_{bin} is the number of energy bins and dE is the bin width of the data set. Average flux was evaluated by summing over the reported energy bins. The $|Rd|$ values for low-energy H ion are 18.7% and 13.6% for BON11 and BON14, respectively. Moreover, as shown in the Fig. 3 for He, O, and Fe, BON14 presents a significant improvement over BON11 especially for energies below 4.0 GeV/n.

In Table 2, the overall average relative difference metrics, Rd and $|Rd|$, are presented for BON11 and BON14. These values were determined by averaging the relative difference metrics over each ion. Individual results for each ion were reported in [10]. The results in Table 2 were obtained by considering the entire GCR measurement database (all ion and energy bins). It is seen in Table 2, that for BON11, the $|Rd|$ value is calculated as 23.7% and $Rd = 17.9\%$. For BON14, these errors are reduced to $|Rd| = 13.0\%$ and $Rd = -0.4\%$. The BON11 model systematically overpredicts the GCR measurement data, whereas BON14 provides a more balanced prediction. More importantly, the overall spread in the new model error was reduced from 23.7% to 13.0%. It should be emphasized that at all energies, BON14 is only a marginally improved fit to the hydrogen GCR data compared with BON11. There is room for improvement since BON14 underpredicts hydrogen GCR data for ~ 8 year-long periods since 1998 (per Fig. 3). A similar underpredicting pattern is observed for He as well.

3. Conclusions

We present the comparison results of BON14 with an updated set of GCR measurements from various balloon, satellite, and space shuttle measurements. The new model LIS parameters were fitted with an updated approach based on the sensitivity study described earlier. This study showed that the GCR ions with energies between 0.5 GeV/n and 4.0 GeV/n account for most of the shielded effective dose.

The overall average Rd value is calculated as 17.9% for the BON11 and -0.4% for the BON14 model, whereas $|Rd|$ is found as 23.7% and 13.0% for BON11 and BON14

Table 2: The average relative difference metrics between the entire GCR database with BON11 and BON14.

	Average [%]	
	Rd	$|Rd|$
BON11	17.9	23.7
BON14	-0.4	13.0

models, respectively. As described in [10], the uncertainty metrics study also revealed that overall the BON14 model has been improved significantly with respect to the previous models (BON10 and BON11) both at low- and high-energy regions. However, it should be noted that the LIS parameters used by BON14 slightly underpredict hydrogen GCR data for most of the years since $\sim$ 1998 (beginning of a solar maximum). We anticipate significant model improvement in the energy region of interest with hydrogen data when the new GCR measurements are available in the future; e.g., AMS-02 measurements. In addition, we will attempt to improve the model by incorporating several physics effects on the GCR particles (e.g., curvature and gradient drifts) which have not been included in the previous BON models.
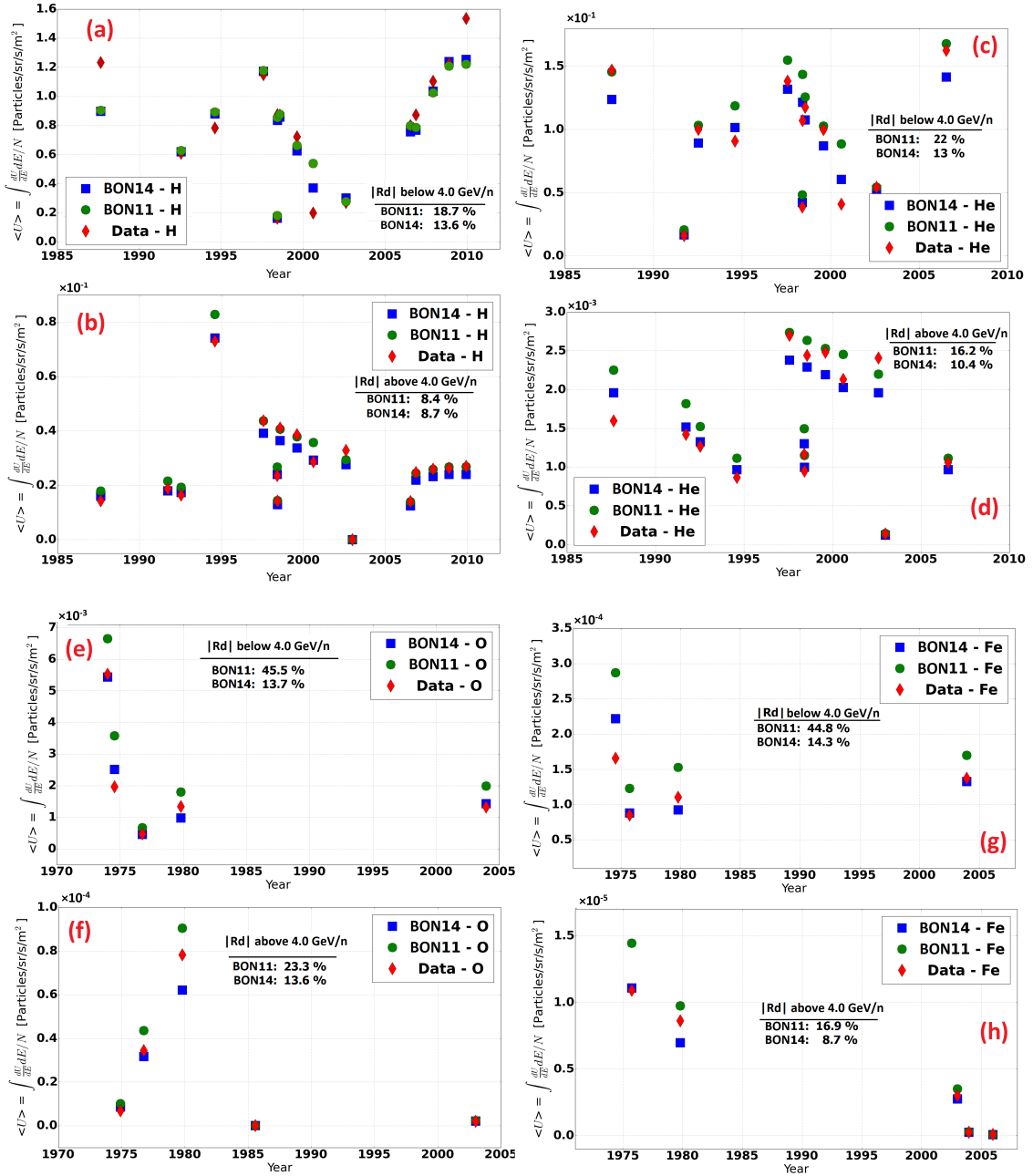
4. Acknowledgment

Figure 3: The average flux values, $< U >$, for H ion: (a) below, (b) above; He: (c) below, (d) above; O: (e) below, (f) above; and Fe: (g) below, (h) above 4.0 GeV/n are shown as a function of measurement date for BON11 and BON14. $|Rd|$ values of the models compared against same GCR database are presented in the legends of the figures.

References

[1] *National Council on Radiation Protection and Measurements (NCRP), Information Needed to Make Radiation Protection Recommendations for Space Missions Beyond Low-Earth Orbit*, Tech. Rep. No. 153, Natl. Counc. on Radiat. Prot. and Meas., Bethesda, Maryland, 2006.

[2] F. A. Cucinotta, M.-H. Y. Kim, and L. J. Chappell, *Space Radiation Cancer Risk Projections and Uncertainties-2012*, Tech. Rep. NASA/TP-2013-217375, (2013).

[3] M. Durante and F. A. Cucinotta, *Physical basis of radiation protection in space travel*, *Rev. Mod. Phys.* **83** (Nov, 2011) 1245–1281.

[4] L. Adams, *Cosmic ray effects in microelectronics*, *Microelectronics Journal* **16** (1985), no. 2 17 – 29.

[5] P. M. O'Neill and G. D. Badhwar, *Single event upsets for Space Shuttle flights of new general purpose computer memory devices*, *IEEE Transactions on Nuclear Science* **41** (Oct., 1994) 1755–1764.

[6] G. D. Badhwar and P. M. O'Neill, *Long-term modulation of galactic cosmic radiation and its model for space exploration.*, *Advances in Space Research* **14** (1994), no. 10 (749 – 757).

[7] G. Badhwar and P. O'Neill, *Galactic cosmic radiation model and its applications*, *Advances in Space Research* **17** (1996), no. 2 7 – 17.

[8] P. O'Neill, *Badhwar-O'Neill 2010 Galactic Cosmic Ray Flux Model; Revised*, *Nuclear Science, IEEE Transactions on* **57** (Dec, 2010) (3148–3153).

[9] P. M. O'Neill and C. C. Foster, *Badhwar-O'Neill 2011 Galactic Cosmic Ray Flux Model Description*, Tech. Rep. NASA/TP-2013-217376, (2013).

[10] P. M. O'Neill, S. Golge, and T. C. Slaba, *Badhwar - O'Neill 2014 Galactic Cosmic Ray Flux Model Description*, Tech. Rep. TP-2015-218569, NASA Technical Report, 2015.

[11] E. N. Parker, *The passage of energetic charged particles through interplanetary space*, *Planetary and Space Science* **13** (1965), no. 1 9 – 49.

[12] L. J. Gleeson and W. I. Axford, *Cosmic rays in the interplanetary medium*, *Astrophysical Journal* **149** (1967) L115.

[13] L. A. Fisk, *Solar modulation of galactic cosmic rays, 2*, *Journal of Geophysical Research* **76** (1971), no. 1 221–226.

[14] T. C. Slaba and S. R. Blattnig, *GCR environmental models I: Sensitivity analysis for GCR environments*, *Space Weather* **12** (2014), no. 4 217–224.

[15] T. C. Slaba and S. R. Blattnig, *GCR environmental models II: Uncertainty propagation methods for GCR environments*, *Space Weather* **12** (2014), no. 4 225–232.

[16] T. C. Slaba, X. Xu, S. R. Blattnig, and R. B. Norman, *GCR environmental models III: GCR model validation and propagated uncertainties in effective dose*, *Space Weather* **12** (2014), no. 4 233–245.

[17] E. C. Stone, A. M. Frandsen, R. A. Mewaldt, E. R. Christian, D. Margolies, J. F. Ormes, and F. Snow, *The advanced composition explorer*, *Space Science Reviews* **86** (1998), no. 1-4 1–22.

[18] J. Alcaraz et al., *Cosmic protons*, *Physics Letters B* **490** (2000), no. 1-2 27–35.

[19] W. Menn et al., *The Absolute Flux of Protons and Helium at the Top of the Atmosphere Using IMAX*, *The Astrophysical Journal* **533** (Apr., 2000) 281–297.

[20] O. Adriani et al., *PAMELA Measurements of Cosmic-Ray Proton and Helium Spectra*, *Science* **332** (Apr., 2011) 69, [arXiv:1103.4055].